Agriculture, Ecosystems and Environment 314 (2021) 107388

Contents lists available at ScienceDirect

Agriculture, Ecosystems and Environment

journal homepage: www.elsevier.com/locate/agee

Soil erosion leads to degradation of hydraulic properties in the agricultural region of Northeast China

Haiqiang Li [a,b], Hansong Zhu [a,b], Xiaorong Wei [a,b,c,*], Baoyuan Liu [b], Mingan Shao [b]

[a] College of Natural Resources and Environment, Northwest A&F University, Yangling, 712100, China
[b] State Key Laboratory of Soil Erosion and Dryland Agriculture on the Loess Plateau, Northwest A&F University, Yangling, 712100, China
[c] CAS center for Excellence in Quaternary Science and Global Change, Xi'an, 710061, China

ARTICLE INFO

Keywords:
Soil erosion
Soil organic matter
Saturated hydraulic conductivity
Soil water retention curve

ABSTRACT

Agricultural erosion leads to degradation of hydraulic properties and further affects agroecosystem hydrological cycling. How such properties respond to intensities of erosion remain unclear, hindering the understanding of the mechanisms behind agroecosystem hydrological cycling. Herein, we investigated the variations in soil hydraulic and physical properties at different slope positions that subjected to various intensities of soil erosion (non-erosion, light erosion, moderate erosion, and heavy erosion) and deposition positions along a maize field in the agricultural region. The average erosion moduli were <200, 700, 1800 and 4200 t km^{-2} a^{-1} at the non-erosion, light erosion, moderate erosion, and heavy erosion sites, respectively. The measured soil properties included soil organic matter, bulk density, saturated hydraulic conductivity (K_s), soil water content, capillary moisture capacity, field capacity, parameters of the soil water retention curve and water-stable aggregates. Our results showed that organic matter, K_s, soil water content, capillary moisture capacity, field capacity and most parameters of soil water retention curve (i.e., θ_r, θ_s and n) decreased, but bulk density increased with soil depth at the eroding and non-erosion sites. Soil erosion decreased organic matter, K_s, soil water content, capillary moisture capacity, field capacity and the ability of soils to retain water but increased soil bulk density. The proportions of aggregates were not affected by soil depth or its interaction with soil erosion, while soil erosion decreased microaggregates but increased macroaggregates. Overall, in this study, agricultural erosion resulted in the degradation of soil hydraulic and physical properties, which may increase the risk of the agricultural ecosystem to suffer drought.

1. Introduction

In arid and semi-arid regions, inter-annual and seasonal variations of rainfall often lead to annual and seasonal soil drought and thus negatively affects the growth of crops in agricultural land (Kume. et al., 2007; Wang et al., 2015a). Meanwhile, in recent years, the frequent occurrence of extreme precipitation events has profoundly accelerated soil erosion (Markus, 2008; Manyevere et al., 2016), changed agricultural hydrological cycles (Chahine, 1992; Lal, 2001; Ouyang et al., 2018), and further decreased stability of agroecosystem (Onet et al., 2019; Xiao et al., 2020). Previous observations indicated that agricultural soil erosion has short-term effects on loss of soil water and long-term effects on reduction of available water content, thereby increasing soil drought in agricultural ecosystem (Lal, 2001; Li et al., 2018; Ouyang et al., 2018). Additionally, soil erosion changes soil hydraulic and physical properties, i.e., soil particle size distribution, bulk density (BD), aggregates size distribution, and unsaturated and saturated hydraulic conductivity (Reganold et al., 1987; Sarapatka et al., 2018; Gu et al., 2018; Borrelli et al., 2018). Such changes will in turn influence rainwater infiltration and surface runoff and thus soil drought (Ouyang et al., 2018). Thus, understanding erosion-induced changes in soil hydraulic and physical properties is imperative for assessing the risks of agricultural ecosystem to suffer drought.

The responses of soil hydraulic and physical properties to soil erosion vary with soil texture (Mamedov and Levy, 2001; Lado et al., 2004; Letey et al., 2001; Wang et al., 2018). It has been reported that fine particles enter macropores and seal surface soils during water erosion (Ben-Hur et al., 2009; Mamedov and Levy, 2001), which reduces porosity, pore size and community (Assouline, 2006; Huang and Bradford, 1993) and water permeability into soils (Ahuja, 1983). The sealed

* Corresponding author at: Xinong Road, #26, Yangling, Shaanxi Province, 712100, China.
E-mail address: xrwei78@163.com (X. Wei).

https://doi.org/10.1016/j.agee.2021.107388
Received 10 December 2020; Received in revised form 15 February 2021; Accepted 28 February 2021
Available online 24 March 2021
0167-8809/

macropores and reduction in soil porosity could result in an increase in BD (Assouline, 2006; Eynard et al., 2004) and thus reduce unsaturated/saturated hydraulic conductivity (Biddoccu et al., 2017; Thomaz, 2017; Sobieraj et al., 2002). Soil compaction by mechanized tillage is also apt to occur in clay soils with high water content, which directly destroys soil structure, reduces porosity, and increases bulk density (Abrol et al., 2016; Bogunović et al., 2018). However, most previous studies have been conducted on soils with low clay content (<20 %) (Larson and Padilla, 1990; Harris and Ragusa, 2001; Sharma and Verma, 1977; Zhao et al., 2018). Therefore, it is urgently needed to understand how soil hydraulic and physical properties respond to agricultural soil erosion in heavy clay soils.

The effects of tillage erosion (Islam and Weil, 2000; Logsdon, 2013; Hong et al., 2017), wind erosion (Belnap and Gillette, 1998; Breshears, 2010; Zhao et al., 2005), and most types of water erosion (Bryan, 2000; Wirtz et al., 2012) on soil physical, chemical and biological properties were intensively investigated in surface soils (0−20 cm). For instance, Zhao et al. (2006) showed that long-term severe wind erosion reduced soil clay content and soil water content and decreased soil fertility at the 0−20 cm depth compared with non-eroded farmland in Inner Mongolia. McDonald et al. (2002) indicated that tillage could result in declines of soil organic carbon and nutrients contents but increase of soil bulk density at a depth of 0−10 cm over 5-year period in the Blue Mountains of Jamaica. Tuo et al. (2018) reported that wind and water erosion increased the spatial variability of soil properties and seriously decreased the nutrient contents in 0−20 soils in sloping fields on the Chinese Loess Plateau. However, the changes in physical and hydraulic properties in deep soils will affect infiltration through soil profiles and have the potential to influence runoff and produce erosion risks. For example, the low soil BD and high saturated hydraulic conductivity in deep soils will favor the drainage of soil water and thus decrease runoff and soil erosion (Choudhary et al., 1997; Ouyang et al., 2018). Similarly, compaction due to mechanical tillage will result in high BD and low saturated hydraulic conductivity (K_s) in deep soils (Arachchi, 2009; Rehder, 1995; Sanford et al., 2008; Sobieraj et al., 2002; Yang et al., 2017) and hence decrease the infiltration of rainwater and increase overland flow (Ouyang et al., 2018). Therefore, the responses of soil properties in deep soils (generally below 30 cm) to erosion at different topographic positions along a transect merit thorough understanding.

In this study, we present the results of the soil hydraulic and physical properties in 0−100 cm soil profiles in sites suffering from various intensities of soil erosion (from non-erosion to heavy erosion) along a cropland transect in Northeast China. The soils were collected to determine soil BD, aggregates size distribution, K_s, soil water retention curves, and soil water parameters. The main objectives of this study were to address how soil hydraulic and physical properties respond to erosion in agroecosystem, and to identify whether such responses vary with soil depth, i.e., surface soil vs. subsoil. Such knowledges are essential for the understanding of agroecosystem hydrological cycling as affected by erosion.

2. Materials and methods

2.1. Study site

The study site was located in Hebei watershed (48°59′-49°03′N, 125°16′-125°21′E) in Heilongjiang Province in Northeast China. According to the description by Li et al. (2019 and 2020), the topography in the study area is characterized by long slopes (up to 2 km) and gentle (1−4°) with an elevation of 310−390 m asl. The study site has a cold and semiarid climate. The mean annual temperature, precipitation and frost-free period is approximately 0.4 °C, 500 mm and 115–120 days, respectively (Hu et al., 2007; Qiu et al., 2021a). The soil in the study site is classified as Mollisols with a texture of clay loam (USDA, 1975). The clay content ranges from 30 % to 49 % (Zhao et al., 2006a, 2006b; Li et al., 2019), allowing us to test the responses in soils with heavy texture.

2.2. Soil sampling

In this study, we established our sampling plots in a maize (*Zea mays* L.) field (900 × 260 m) that was converted from forest for crop production approximately 60 years ago, and it is near the JiuSan Soil and Water Conservation Experimental Station of Beijing Normal University. Soil erosion in the area has been intensively studied and monitored by scientists since the early 2000s (Dong et al., 2019; Wu et al., 2008; Zhang et al., 2007; Li et al., 2012). In the harvest season of 2017 (early October), following previous observational data, we selected four soil erosion intensities, i.e., non-erosion sites (NE), light erosion sites (LE), moderate erosion sites (ME), and heavy erosion sites (HE), at four slope positions along a cropland transect (Fig. 1) (Li et al., 2020; Qiu et al., 2021a). The erosion muduli was smaller than 200 t km^{-2} a^{-1} at the NE. The average erosion moduli were 700, 1800 and 4200 t km^{-2} a^{-1} at the LE, ME and HE, respectively (unpublished data from Beijing Normal University). In addition, we also selected the deposition sites (DS) at the bottom of the slope to assess the effects of sediment deposition on soil properties according to the observational data (Dong et al., 2019; Wu et al., 2008; Zhang et al., 2007; Li et al., 2012).

Three subplots (10 × 10 m) as replicates at each of the different slope positions were established for soil sampling. The sampling plots in each erosion phase were randomly established and were at least 10 m apart from each other. According to sampling method described by Li et al. (2019), in each subplot, undisturbed soil cores were collected from soil depths of 0−15, 15−30, 30−50, 50−70 and 70−100 cm using 100 cm^3 stainless-steel cylinders (with 5.0-cm height). Additionally, five disturbed soil samples were collected from each depth within each subplot using a 5.0-cm diameter soil auger and were combined to form a composite sample. The undisturbed soil cores and composite soil samples were carefully taken to the laboratory. The undisturbed soil cores were used to determine saturated hydraulic conductivity (K_s, cm d^{-1}), capillary moisture capacity (CMC, %), field capacity (FC, %), the soil water retention curve (SWRC) and bulk density (BD, g cm^{-3}). The composite samples were used for measurement of the soil organic matter (SOM) content, soil water content (SWC), and water-stable aggregates (Li et al., 2019).

2.3. Measurements of soil hydraulic and physical properties

A small fraction of each composite sample was used to determine SWC by oven-drying at 105 °C for 24 h. The remaining composite samples were air-dried and then ground to pass through 8.0-, 2.0- and 0.25-mm sieves to analyze aggregates, particle composition, and organic matter content, respectively. The SOM was measured using the Walkley-Black method (Nelson et al., 1996). The water-stable aggregate distribution was analyzed by a revised wet-sieving method (Six et al., 1998; Li et al., 2019). The four aggregate size classes, i.e., large macroaggregate (LMA, >2 mm), small macroaggregate (SMA, 0.25−2 mm), microaggregate (MI, 0.25−0.053 mm), and silt + clay fraction (SC, <0.053 mm), were separated. This measurement procedures of water-stable aggregate have been described in detail by Li et al. (2019). Although this method might overestimate the proportion of small size aggregates due to the excessive disturbance of this fraction, we reported results from this most commonly used method so that our results would be comparable with others.

The undisturbed soil cores firstly were saturated at room temperature for 24 h and then the K_s of the undisturbed soil cores were measured with the falling-head method based on Darcy's law (Klute and Dirksen, 1986). According to the measurement procedures of FC and CMC described in detail by Li et al. (2019), the FC and CMC were determined using the same soil core samples after the measurement of K_s.

The SWRC for each undisturbed soil core was determined by the centrifugation method adapted by Reatto et al. (2008). For further details of the centrifuge method for determining soil water retention properties, see Li et al. (2019). The van Genuchten model (van

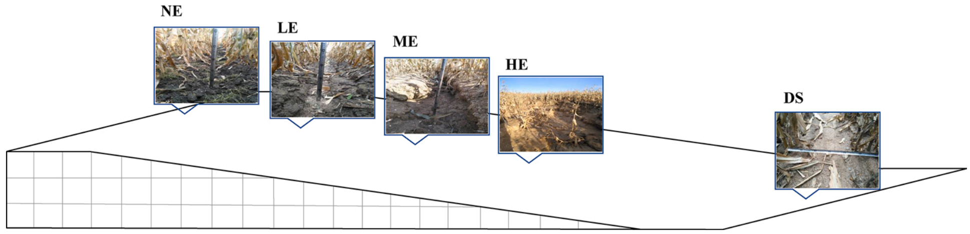

Fig. 1. Location of each intensity of soil erosion and deposition at five slope positions along a cropland transect. NE: non-erosion site; LE: light erosion site; ME: moderate erosion site; HE: heavy erosion site; DS: deposition site.

Genuchten 1984) was used to fit the measured soil water retention data to the suction pressures of 1–800 kPa, thereby deriving the parameters of VG equation (i.e., θ_r, θ_s, α, and n) for each undisturbed soil core (Li et al., 2019).

Generally, the CMC and FC could also be obtained by fitting the soil water retention curve (SWRC) with head pressures of 10 and 33 kPa (Wilkinson and Klute, 1959; Chen and Wagenet, 1992), respectively. The measured CMC and FC were positively correlated with the calculated CMC and FC, respectively. For example, in this study, we found a positive relationship between the measured CMC and FC and the calculated CMC and FC, respectively, and the metrics obtained by direct measurement and fitting SWRC had similar response patterns to soil erosion. In our study, most soil metrics we present were directly measured; herein, we provide the measured CMC and FC rather than calculated ones, but we do not intend this as an indication that measured CMC and FC are preferable to calculated ones.

2.4. Statistical analysis

In this study, the thickness of the Mollisols layer was 40−50 cm at the NE and 30−40 cm at the eroding sites. Given that we sampled soils from depths of 0−15, 15−30, 30−50, 50−70 and 70−100 cm, the difference in the thickness of the Mollisols layer among the sites should have minimum influence on the effects of soil depth or its interaction with erosion. Therefore, we neglected this difference in Mollisols layer thickness when analyzing the effects of erosion. Two-way analysis of variance (ANOVA) was used to test the effect of slope position (soil erosion), soil depth, and their interactive effects on soil hydraulic and physical properties. Pearson's correlation analyses were conducted to establish relationships among soil properties. The Shapiro-Wilk test was used to test for normality, and data were log-transformed when necessary. All statistical analyses were conducted using SPSS 13.0.

3. Results

3.1. Effects of erosion on soil organic matter, bulk density and saturated hydraulic conductivity

The SOM, BD and K_s were significantly affected by soil depth, soil erosion, and their interactions (Table 1). Generally, SOM was not affected by soil depth at the DS (24.9-34.6 g kg^{-1} among soil depths) but decreased significantly with soil depth in NE and eroding sites at the 0−50 cm depth and remained relatively constant below 50 cm, ranging from 39.6 g kg^{-1} at the 0−15 cm depth to 11.8 g kg^{-1} at the 30−50 cm depth and 2.5 g kg^{-1} at the 70−100 cm depth (Fig. 2a). Soil erosion resulted in a significant decrease in SOM compared with that at the NE, and the highest decrease occurred at the 0−30 cm depth. When compared with the NE, the LE, ME and HE resulted in 7.0, 20.1, and 20.7 g kg^{-1} decreases in SOM in the 0−15 cm soils and 2.8, 14.3, and 16.3 g kg^{-1} decreases in the 15−30 cm soils, respectively (Fig. 2a). For soils at the 30−70 cm depths, SOM was significantly higher at the DS than at either the NE or eroding sites (3.4 to 27.3 g kg^{-1}), indicating the burial of SOM at the DS.

Similar to SOM, K_s significantly decreased with soil depth, with a value of 7.9 cm d^{-1} at the 0−15 cm depth but 3.8 cm d^{-1} at the 15−30 cm depth and 2.2 cm d^{-1} at the 70−100 cm depth when averaged across the NE, eroding sites and DS. Moreover, soil erosion significantly decreased K_s, and this effect mainly occurred at the 0−70 cm depth. For example, the K_s in the 0−70 cm soils from the LE, ME and HE was 2.1–7.01, 3.3–7.3, and 2.43-13.2 cm d^{-1} lower, respectively, than the K_s at the NE (Fig. 2c). The K_s at the 15−70 cm depth from the DS (4.1 cm d^{-1} to 6.8 cm d^{-1}) was significantly higher than that from the eroding sites (0.9 cm d^{-1} to 4.1 cm d^{-1}) (Fig. 2c).

In contrast to SOM and K_s, soil BD increased with soil depth and erosion (Fig. 2b). When averaged across the NE, eroding sites and DS, BD increased from 1.5 g cm^{-3} at the 0−15 cm depth to 1.6 g cm^{-3} at the 15−30 cm depth and 1.73 g cm^{-3} at the 70−100 cm depth. The BD at the LE, ME and HE at the 0−70 cm depth was 0.09−0.22, 0.15−0.38 and 0.17−0.41 g cm^{-3} higher than that at the NE, respectively (Fig. 2b). Moreover, the averaged BD at the 15−70 cm depth was 0.10−0.37 g

Table 1
Results of variance analysis (*F*-values and *P*-values) for the effects of soil erosion and soil depths on soil properties.

	SWC	BD	FC	CMC	K_s	LMA	SMA	MI	SC	θ_r	θ_s	α	n	SOM
F														
Soil erosion	42.85	30.32	66.18	57.70	14.05	21.61	17.71	21.67	8.91	14.85	36.63	25.96	24.21	14.82
Soil depth	5.88	21.65	24.31	23.33	11.41	0.44	3.39	1.59	2.21	11.87	30.63	26.78	17.30	21.95
Soil erosion × soil depth	0.70	3.60	8.59	4.45	2.72	0.28	0.32	0.28	0.40	2.18	2.63	3.76	2.61	2.17
P														
Soil erosion	**< 0.01**	**< 0.01**	**< 0.01**	**< 0.01**	**< 0.01**	**< 0.01**	**< 0.01**	**< 0.01**	**< 0.01**	**< 0.01**	**< 0.01**	**< 0.01**	**< 0.01**	**< 0.01**
Soil depth	**< 0.01**	**< 0.01**	**< 0.01**	**< 0.01**	**< 0.01**	0.78	**0.02**	0.20	0.09	**< 0.01**	**< 0.01**	**< 0.01**	**< 0.01**	**< 0.01**
Soil erosion × soil depth	0.77	**0.04**	**< 0.01**	**< 0.01**	**0.01**	0.99	0.99	0.99	0.97	**0.04**	**0.01**	**< 0.01**	**0.01**	**0.04**

SWC: soil water content; BD: bulk density; FC: field capacity; CMC: capillary moisture capacity; K_s: saturated hydraulic conductivity; LMA: large macroaggregate (> 2 mm); SMA: small macroaggregate (0.25−2 mm); MI: microaggregate (0.053−2 mm); SC: silt + clay fraction (< 0.053 mm); θ_r: residual soil water content; θ_s: saturated soil water content; α: scaling parameter related to the inverse of the air entry pressure; n: curve-shape parameters related to the pore size distribution; SOM: soil organic matter.

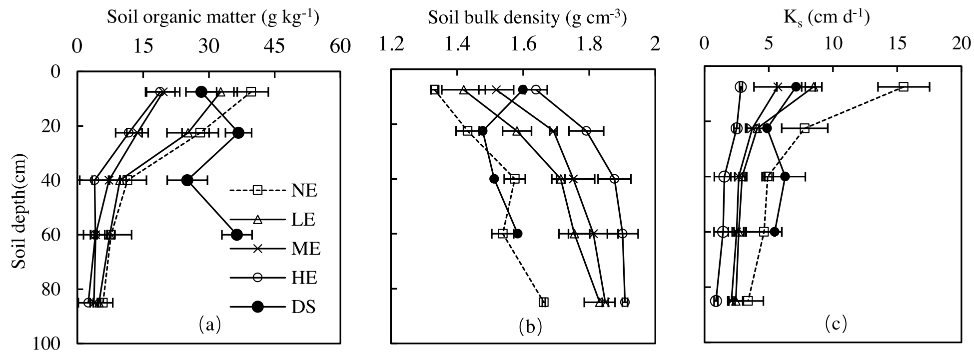

Fig. 2. The soil organic matter, bulk density and saturated hydraulic conductivity (K_s) along soil profiles as affected by agricultural soil erosion. The error bars are two standard errors of the means. NE: non-erosion site; LE: light erosion site; ME: moderate erosion site; HE: heavy erosion site; DS: deposition site.

cm^{-3} higher at the eroding sites than at the DS.

3.2. Effects of erosion on water-stable aggregates

The proportions of aggregates of different sizes were significantly affected by soil erosion but were not affected by soil depth or its interaction with soil erosion, except for SMA, which was significantly higher at the 70−100 cm depth (67.2–79.9 %) than at the 0−70 cm depth (55.6–78.1 %) (Table 1, Fig. 3a). When averaged across the NE, eroding sites and DS, the ranges of the proportions of LMA, SMA, MI, and SC were 5.1–7.5 %, 63.6–74.2 %, 12.0−20.0%, and 6.3–8.1 %, respectively, across the 0−100 cm depths.

Soil erosion increased the proportions of LMA and SMA but decreased the proportion of MI in the 0−100 cm soils (Fig. 3), and most of these effects were consistent with soil depth ($P > 0.05$ for interaction between soil depth and erosion, Table 1). When compared with the NE, LMA was 1.0–4.7, 3.9–8.1, and 5.2–9.4 % higher at the LE, ME and HE, respectively, and SMA was 2.1–8.3, 6.5–10.5, and 11.1–22.5 % higher, respectively. However, MI was 6.1–11.8, 8.0–15.8 and 11.7–23.6 % lower, respectively (Fig. 3). The SC was smaller at the ME and HE (5.9–8.2 % and 4.9–7.8 %) but higher (9.1–13.5 %) at the LE than at the NE (7.6–8.6 %). Moreover, SOM content for total soil was negatively correlated with the proportion of LMA, SMA, and SC but positively correlated with MI (Table 1, $P > 0.05$).

The soils at the DS generally had lower proportions of LMA and SMA than those at the HE but higher proportions than those at the NE and LE. The MI and SC at the DS were higher than those at the HE but lower than those at the NE, LE and ME (Fig. 3).

3.3. Effects of erosion on the parameters of soil water retention curve

The parameters (θ_r, θ_s, α and n) describing soil water retention curves (SWRC) were significantly affected by soil depth, soil erosion and their interactions (Table 1). Generally, θ_r, θ_s and n decreased, while α increased with increasing soil depth (Fig. 4). For example, when averaged across the NE, eroding sites and DS, θ_r, θ_s and n decreased from 0.087 cm^3 cm^{-3}, 0.45 cm^3 cm^{-3} and 1.4 at the 0−15 cm depth to 0.082 cm^3 cm^{-3}, 0.41 cm^3 cm^{-3} and 1.33 at the 15−30 cm depth and 0.072 cm^3 cm^{-3}, 0.35 cm^3 cm^{-3} and 1.2 at the 70−100 cm depth, respectively. Correspondingly, the value of α increased from 0.0127 cm^{-1} at the 0−15

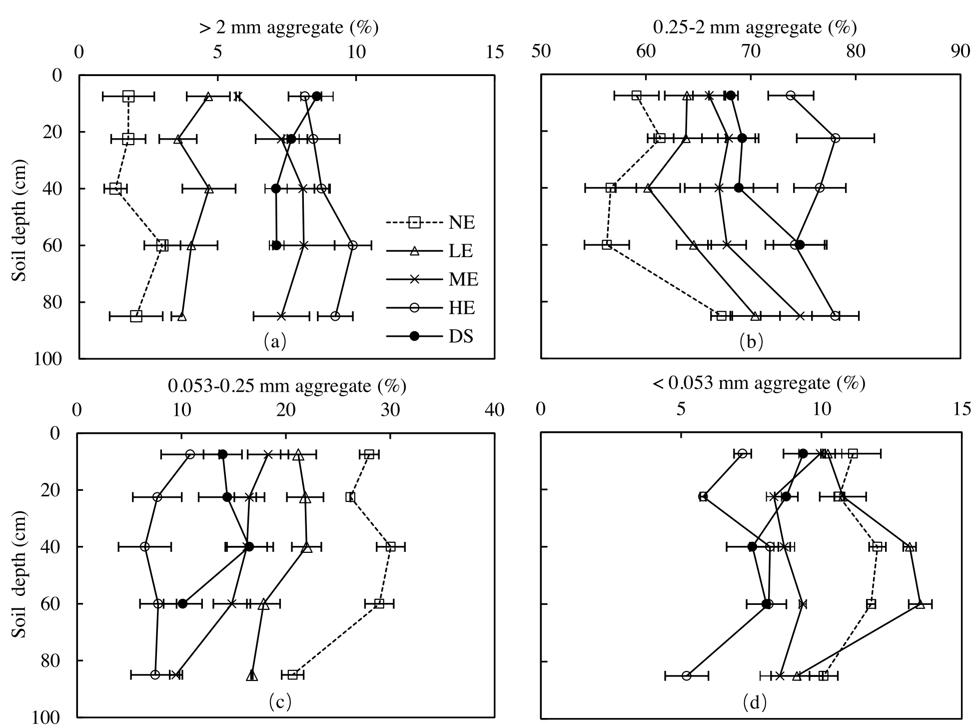

Fig. 3. The distribution of water-stable aggregates along soil profiles as affected by agricultural soil erosion. The error bars are two standard errors of the means. NE: non-erosion site; LE: light erosion site; ME: moderate erosion site; HE: heavy erosion site; DS: deposition site.

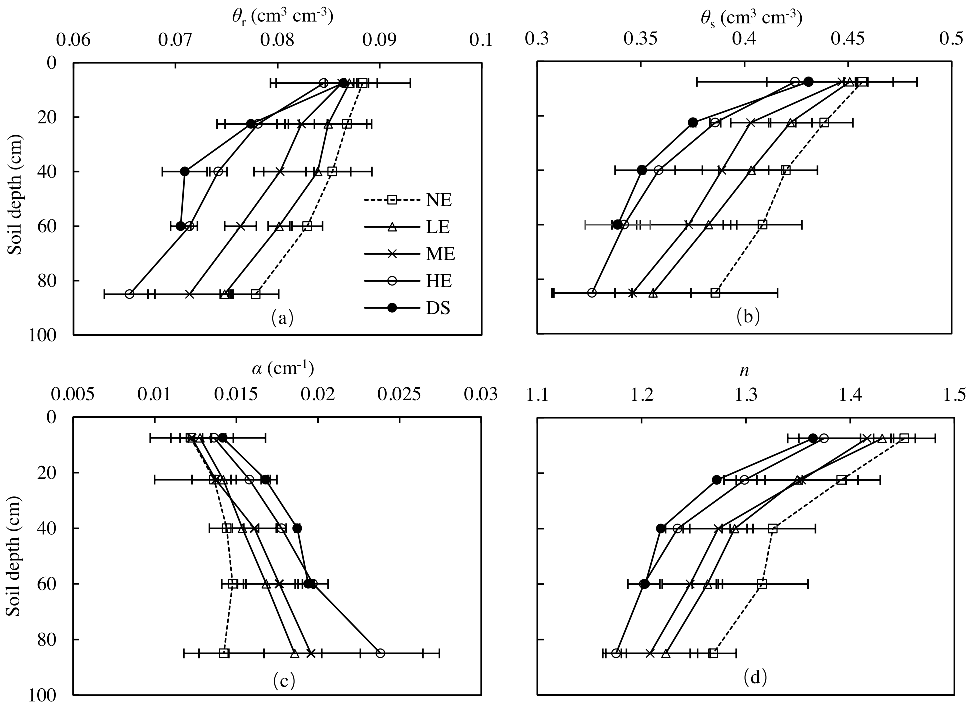

Fig. 4. The parameters (θ_r, θ_s, α and n) describing the soil water retention curves (SWRCs) along soil profiles as affected by agricultural soil erosion. The error bars are two standard errors of the means. NE: non-erosion site; LE: light erosion site; ME: moderate erosion site; HE: heavy erosion site; DS: deposition site; θ_r: residual soil water content; θ_s: saturated soil water content; α: scaling parameter related to the inverse of the air entry pressure; n: curve-shape parameters related to the pore size distribution.

cm depth to 0.0145 cm^{-1} at the 15–30 cm depth and 0.0223 cm^{-1} at the 70–100 cm depth.

Generally, θ_r, θ_s and n were significantly lower, whereas α was significantly higher at the eroding sites than at the NE. For instance, in the 0–100 cm soils, θ_r was 0.001–0.002, 0.002–0.007 and 0.4-1.2 cm^3 cm^{-3} lower at the LE, ME and HE than at the NE, respectively, θ_s was 0.006–0.03, 0.01–0.04 and 3.3-6.0 cm^3 cm^{-3} lower, and n was 0.021–0.053, 0.036–0.069 and 0.077–0.114 lower. On the contrary, α was 0.0005–0.0043, 0.003–0.0053 and 0.0014–0.0096 cm^{-1} higher. Moreover, most of these effects were greater at depths of 50–70 cm than at the other depths.

The values of θ_r, θ_s, and n at the 0–15 cm depth were smaller at the DS than those at the eroding sites, while the values at the 15–70 cm depth were greater than those at the eroding sites (Fig. 4). α at the DS was greater than those at the LE and ME at the 0–15 cm depth but was smaller than those at the eroding sites at the 15–70 cm depth (Fig. 4).

3.4. Effects of erosion on soil water conditions

The SWC consistently decreased with soil depth at each site (Table 1), with values of 0.244 and 0.238 cm^3 cm^{-3} at depths of 0–15 and 15–30 cm, respectively, but 0.181 cm^3 cm^{-3} at depths of 70–100 cm. Soil erosion resulted in a significant decrease in SWC, with 0.051–0.112, 0.053–0.132 and 0.161–0.224 cm^3 cm^{-3} lower SWC at the LE, ME and HE than at the NE at the 0–70 cm depth, respectively (Fig. 5a). The SWC at the DS was 0.003–0.09 cm^3 cm^{-3} lower than that at the NE but 0.04–0.210 cm^3 cm^{-3} higher than that at the eroding sites (Fig. 5a).

The FC and CMC were significantly affected by soil depth, soil erosion and their interaction (Table 1). For the NE and eroding sites, both FC and CMC decreased with soil depth, with mean values of 0.275 cm^3 cm^{-3} and 0.418 cm^3 cm^{-3} in the 0–50 cm soils and 0.22 cm^3 cm^{-3} and 0.371 cm^3 cm^{-3} in the soils below 50 cm when averaged across the sites, respectively. For the DS, however, the mean values of FC and CMC were lower in the 0–50 cm soils (0.258 cm^3 cm^{-3} and 0.408 cm^3 cm^{-3}, respectively) than in the 50–70 cm soils (0.35 cm^3 cm^{-3} and 0.466 cm^3 cm^{-3}, respectively, Fig. 5b and c). Similar to SWC, FC and CMC significantly decreased by erosion (Fig. 5). For example, at the 0–100 cm depth, the FC was 0.013–0.133, 0.046–0.205 and 0.115–0.226 cm^3 cm^{-3} lower at the LE, ME and HE than at the NE, respectively, and the CMC was 0.019–0.109, 0.067–0.147 and 0.095–0.15 cm^3 cm^{-3} lower than that at the NE, respectively. The FC and CMC were 0.172–0.178

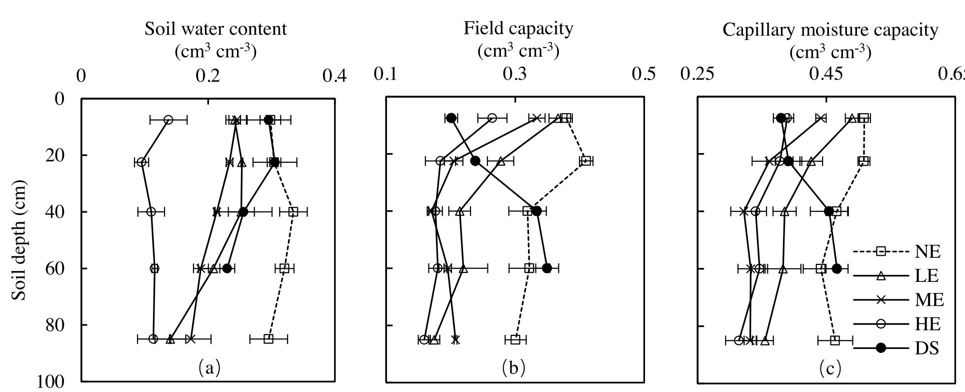

Fig. 5. Soil water content, field capacity and capillary moisture capacity along soil profiles as affected by agricultural soil erosion. The error bars are two standard errors of the means. NE: non-erosion site; LE: light erosion site; ME: moderate erosion site; HE: heavy erosion site; DS: deposition site.

cm^3 cm^{-3} and 0.117–0.129 cm^3 cm^{-3} lower at the DS than that at the NE at the 0–30 cm depth (P < 0.05), respectively, but were not significantly different between the two sites at the 30–70 cm depth (Fig. 5). Moreover, the FC and CMC at the DS were relatively lower than those at the eroding sites at the 0–15 cm depth but higher at the 30–70 cm depth (Fig. 5). Therefore, soil erosion and deposition altered the availability of soil water in this Mollisols.

4. Discussion

4.1. Effects of erosion on soil organic matter, bulk density and saturated hydraulic conductivity

The significantly lower content of SOM at the eroding sites compared with the NE observed in this study was mainly due to the loss of soils, which led to the transportation of SOM and nutrients from the surface soils out of the eroding sites (Osman, 2013; Zhao et al., 2018; Sarapatka et al., 2018; Qiu et al., 2021b). For example, it has been reported that soil erosion results in the loss of 23.7–120 Pg soil yr^{-1} and 0.5–3.7 Pg SOM y^{-1} in agricultural soils at the global scale (Doetterl et al., 2012). Borrelli et al. (2018) reported a loss of 0.16 ± 0.01 Pg soil yr^{-1} and 24.99 Tg SOM yr^{-1} associated with runoff and sediments in Europe. Our results were consistent with previous observations that SOM is usually higher in sediments than in soils from eroding sites (Liu et al., 2003; Yadav and Malanson, 2009). In addition, SOM in eroded soils is exposed to air and microbes and is apt to decompose after erosion (Garciapausas et al., 2008) because erosion destroys soil structure and thus the physical protection of SOM from decomposition (Sarapatka et al., 2018). For instance, Harden et al. (1999) found that erosion resulted in an increase in the decomposition of SOM in the eroding croplands of Mississippi. Furthermore, the decomposition rate of SOM at the eroding sites was up to 2 orders of magnitude higher than that at the NE or DS (Stallard, 1998; Berhe et al., 2007 and 2012). The higher decomposition rate at the eroding sites might provide an alternative explanation for the lower SOM content compared with that at the NE and DS (Wang et al., 2013; Qiu et al., 2021b).

We observed an accumulation of SOM at the DS (Fig. 2), mainly due to the deposition of SOM associated with sediments at this site. Previous studies have demonstrated that more than 70 % of eroded soils and associated SOM are deposited in flat or concave areas of a toposequence (Stallard, 1998; Yoo et al., 2005) and are progressively buried with original material (Berhe et al., 2007 and 2012). Furthermore, the decomposition of SOM will significantly decrease after burial at the DS because of high soil water (Bryant et al., 1998), poor aeration (Zibilske and Materon, 2005), and low temperatures (Risch et al., 2007). This lower decomposition rate could result in a decrease in SOM loss and thus favor the accumulation of SOM at the DS.

In this study, soil BD increased while K_s decreased with soil depth at both the eroding sites and NE (Fig. 2). This profile distribution pattern was attributed to the mechanical compaction that resulted in the reduction of soil porosity in deep soils and was consistent with previous observations in croplands in the Taleghan watershed of Tehran Province, Iran (Haghighi et al., 2010), and the West of Oldenburg, Germany (Bormann and Klaassen, 2008).

The significantly higher soil BD at the eroding sites was primarily due to the severe losses of surface soils and SOM within surface soils compared with the NE (Table 2). Generally, changes in SOM could contribute to the response of soil BD to erosion. The accumulation of SOM often increases soil porosity and thus decreases soil BD, while the loss of SOM often has the opposite influences (Jiang et al., 2018; Haghighi et al., 2010; Mamedov and Levy, 2001; Ben-Hur et al., 2009; Li et al., 2016). This explanation was supported by our results that soil BD was negatively related to SOM (Table 2) and that SOM was significantly lower at the eroding sites than at the NE (Fig. 2). In addition, erosion also transports surface soils out of eroding sites and thus exposes subsoils with higher BD (Quinton et al., 2010).

The decrease in K_s by erosion (Fig. 2) could be ascribed to the loss of SOM and increase in BD at the eroding sites (Table 2, Fig. 2). Such changes in SOM and BD will decrease soil porosity (Jiang et al., 2019; Wei et al., 2017; Nie et al., 2018; Mamedov and Levy, 2001; Li et al., 2016; Scheffler et al., 2011) and thus K_s (Reichert et al., 2014), as supported by our observation that soil K_s increased with SOM but decreased with soil BD (Tables 1 and 2, Fig. 2). In contrast, the higher K_s at the DS compared with the other sites was attributed to the accumulation of SOM and coarse particles (silt + sand) and lower soil BD.

4.2. Effects of erosion on water-stable aggregates

In this study, soil erosion resulted in increases in LMA and SMA but a decrease in MI at the 0–100 cm depth (Fig. 3), probably due to the preferential transport of small size aggregates from the eroding sites but deposition at the DS. Our explanation about the influences of soil erosion on the redistribution of LMA, SMA and MI was supported by our observation that the SOM content for the total soil was positively correlated with MI within eroded soils (P > 0.05). The mechanism for the effects of soil erosion on aggregates in the Mollisols was different from those in other soils, i.e., loess soils. For loess soils, soil aggregates are dispersed by erosion and then transported out of eroding sites (Wang and Shi, 2015). For example, Algayer et al. (2014) showed that soil erosion resulted in the breakdown of macroaggregates and thus a decrease in LMA and SMA but an increase in MI and SC on the Loess Plateau. Such negative effects of erosion on LMA and SMA were also observed in soils with relatively lower clay contents, e.g., humic loamy soils (Le Bissonnais, 1996), Ultisols (Ma et al., 2014; Yan et al., 2008)

Table 2
Pearson's correlation coefficients among soil properties under different soil erosion intensities in the agricultural region of Northeast China (n = 70).

	FC	CMC	K_s	LMA	SMA	MI	SC	θ_r	θ_s	α	n	SOM
BD	**−0.89****	**−0.93****	**−0.81****	**0.49****	**0.52****	**−0.57****	**−0.32***	**−0.81****	**−0.91****	**0.79****	**−0.84****	**−0.76****
FC		**0.97****	**0.76****	**−0.58****	**−0.52****	**0.59****	**0.34***	**0.78****	**0.84****	**−0.72****	**0.81****	**0.68****
CMC			**0.79****	**−0.56****	**−0.53****	**0.60****	**0.33***	**0.79****	**0.89****	**−0.75****	**0.84****	**0.70****
K_s				**−0.43****	**−0.37****	**0.41****	**0.29***	**0.57****	**0.72****	**−0.52****	**0.73****	**0.72****
LMA					**0.65****	**−0.80****	**−0.58****	**−0.59****	**−0.54****	**0.51****	**−0.36****	−0.17
SMA						**−0.95****	**−0.70****	**−0.55****	**−0.53****	**0.52****	**−0.47****	−0.2
MI							**0.56****	**0.59****	**0.59****	**−0.55****	**0.50****	0.23
SC								**0.42****	**0.32***	**−0.38****	0.20	−0.07
θ_r									**0.87****	**−0.87****	**0.60****	**0.51****
θ_s										**−0.88****	**0.87****	**0.69****
α											**−0.71****	**−0.62****
n												**0.82****

BD: bulk density; FC: field capacity; CMC: capillary moisture capacity; K_s: saturated hydraulic conductivity; LMA: large macroaggregate (> 2 mm); SMA: small macroaggregate (0.25–2 mm); MI: microaggregate (0.053–2 mm); SC: silt + clay fraction (< 0.053 mm); θ_r: residual soil water content; θ_s: saturated soil water content; α: scaling parameter related to the inverse of the air entry pressure; n: curve-shape parameters related to the pore size distribution; SOM: soil organic matter. A bold value indicates statistical significance. ** Coefficient is significant at P < 0.01 level.

and loamy sand soils (Saygin, et al., 2012). However, for Mollisols, the clay content is high (31–49 %), and soil particles are strongly aggregated. Soil erosion is not apt to result in the breakdown of LMA and SMA due to the strong association of soil particles with high clay content (Denef et al., 2002; Wagner et al., 2010; Bhattacharyya et al., 2009). The effects of soil erosion on aggregate size distribution were thus mainly exerted by transporting small size aggregates and hence resulted in a greater proportion of LMA and SMA at the eroding sites. This mechanism was consistent with the observation that erosion results in a greater loss of MI in heavy clay soils (i.e., Mollisols) (Opara, 2009; Le Bissonnais, 1996). Our explanation of the aggregate response to erosion was supported by the results that the DS had lower proportions of LMA and SMA but higher proportions of MI relative to the HE (Fig. 3). Therefore, the effects of soil erosion on aggregate size distribution were largely dependent on soil texture.

4.3. Effects of erosion on the parameters of soil water retention curve

In comparison to those at the eroding sites and DS, the averaged θ_r, θ_s and n were significantly higher whereas the α was lower at the NE (Fig. 4). These responses were mainly attributed to the decreased SOM and increased BD by soil erosion, as SWRC are determined by soil porosity and soil pore-size distribution (Hartmann et al., 2009). Generally, the lower BD and higher SOM result in higher soil porosity (Mamedov et al., 2001; Mamedov and Levy, 2001; Li et al., 2016; Wei et al., 2017; Ben-Hur et al., 2009) and water penetration and retention capacity (Biddoccu et al., 2017; Thomaz, 2017), and thus increase θ_r and θ_s but decrease α (Wang et al., 2015b). In this study, we found that θ_r, θ_s and n were negatively correlated with BD ($P < 0.01$) but positively correlated with SOM ($P < 0.01$) (Table 2), while α was negatively correlated with SOM content ($P < 0.01$) but positively correlated with soil BD ($P < 0.01$) (Table 2), supporting this explanation.

4.4. Effects of erosion on soil water

The decreases in soil water (SWC, CMC and FC, Fig. 5) by erosion were associated with the changes in soil physical properties. Soil erosion led to a higher BD and a lower K_s at the eroding sites than at the NE (Fig. 2), which decreased the infiltration of rainwater into the deep soils but increased the runoff of rainwater from the eroding sites. The water stored in the soils was therefore smaller at the eroding sites than at the NE (Fig. 5). Additionally, the losses of SOM and MI fraction but the increase in soil BD by soil erosion (Fig. 2 and 3) decreased the capillary porosity and total porosity (Li et al., 2016; Cournane et al., 2011), which resulted in a reduction in the retention capacity of water (θ_r, θ_s and n of SWRC, Fig. 4). Such changes decreased the capacity of the soils to retain water at the eroding sites, and thus had lower soil water (SWC, FC, and CMC, Fig. 5). Our observations of the differences in soil water between the eroding sites and NE were consistent with previous works from the Loess Plateau in China (Qiu et al., 2001), Wisconsin in the USA (Hendrix et al., 1992) and Ishigaki Island in Japan (Nagumo et al., 2006).

4.5. Response of hydraulic and physical properties in deep soil to erosion

One of the surprising results of this study is that soil erosion can have significant influences on soil hydraulic and physical properties in deep soils (below 30 cm). The possible reason is the interaction of tillage with erosion. On the one hand, erosion mostly could transport the relatively rich surface soils and expose poor subsoils. On the other hand, at the studied sites, the tillage depth was approximately 30 cm. The differences in SOM and soil physical properties between the eroding sites and NE were generally higher in topsoil (0−30 cm) than in deep soil (below 30 cm). However, the difference in the SWRC parameters between the eroding sites and non-erosion sites was greater in deep soil than in topsoil (Fig. 4). Although the mechanism behind such interaction is unknown, these results suggested that soil erosion enhanced the effects of mechanical tillage on soil hydraulic and physical properties in Northeast China. The degradation of hydrological and physical properties in deep soils could in turn further increase the risk of surface soils experiencing erosion.

5. Conclusions

In this study, we addressed the changes in soil hydraulic and physical properties at the non-erosion sites, eroding sites and deposition sites along a cropland transect to better understand how erosion influences agroecosystem hydrological processes. The results demonstrated significant effects of soil erosion, soil depth and their interaction on SOM, BD, SWC, CMC, FC, K_s and SWRC parameters. The SOM, K_s, SWC, FC, CMC, MI and most SWRC parameters (i.e., θ_r, θ_s and n) at the eroding sites decreased, but BD at the eroding sites increased with soil erosion. The higher BD and lower K_s and SWRC parameters (i.e., θ_r, θ_s and n) at the eroding sites may be attributed to the compaction of tillage management and loss of SOM with soil erosion. In addition, the proportions of aggregates were significantly influenced by soil erosion but were not affected by soil depth or its interaction with soil erosion. Erosion increased the proportion of macroaggregates compared with the non-erosion sites, probably due to the preferential losses of MI and SC at the eroding sites. We also showed that soil erosion could have significant effects on soil hydraulic and physical properties in deep soils (>30 cm). Herein, soil erosion resulted in the degradation of soil hydraulic and physical properties in a sloping cropland and further affected the agroecosystem hydrological cycling in agricultural region of Northeast China, due to the interaction of erosion (water erosion, wind erosion and/or tillage erosion) and mechanized tillage (compaction).

Declaration of Competing Interest

The authors declare that they have no known competing financial interests or personal relationships that could have appeared to influence the work reported in this paper.

Acknowledgments

This work was supported by the National Key Research and Development Program (No. 2018YFC0507001), National Natural Science Foundation of China (41977068 and 41622105), and the Programs from Chinese Academy of Sciences (QYZDB-SSW-DQC039).

Appendix A. Supplementary data

Supplementary material related to this article can be found, in the online version, at doi:https://doi.org/10.1016/j.agee.2021.107388.

References

Abrol, V., Ben-Hur, M., Verheijen, F.G.A., Keizer, J.J., Martins, M.A.S., Tenaw, H., 2016. Biochar effects on soil water infiltration and erosion under seal formation conditions: rainfall simulation experiment. J. Soils Sediments 16 (12), 2709–2719. https://doi.org/10.1007/s11368-016-1448-8.

Algayer, B., Wang, B., Bourennane, H., Zheng, F.L., Duval, O., Li, G.F., Le Bissonnais, Y., Darboux, F., 2014. Aggregate stability of a crusted soil: differences between crust and sub-crust material, and consequences for interrill erodibility assessment: an example from the Loess plateau of China. Eur. J. Soil Sci. 65 (3), 325–335. https://doi.org/10.1111/ejss.12134.

Arachchi, L.P.V., 2009. Effect of deep ploughing on the water status of highly and less compacted soils for coconut (Cocos nucifera L.) production in Sri Lanka. Soil Tillage Res. 103 (2), 350–355. https://doi.org/10.1016/j.still.2008.10.025.

Belnap, J., Gillette, D.A., 1998. Vulnerability of desert biological soil crusts to wind erosion: the influences of crust development, soil texture, and disturbance. J. Arid Environ. 39 (2), 130–142. https://doi.org/10.1006/jare.1998.0388.

Ben-Hur, M., Yolcu, G., Uysal, H., Lado, M., Paz, A., 2009. Soil structure changes: aggregate size and soil texture effects on hydraulic conductivity under different saline and sodic conditions. Soil Res. 47 (7), 688–696. https://doi.org/10.1071/sr09009.

Berhe, A.A., 2012. Decomposition of organic substrates at eroding vs. Depositional landform positions. Plant Soil 350 (1–2), 261–280. https://doi.org/10.1007/s11104-011-0902-z.

Berhe, A.A., Harte, J., Harden, J.W., Torn, M.S., 2007. The significance of erosion-induced terrestrial carbon sink. Bioscience 57 (4), 337–346. https://doi.org/10.1641/b570408.

Bhattacharyya, R., Prakash, V., Kundu, S., Srivastva, A.K., Gupta, H.S., 2009. Soil aggregation and organic matter in a sandy clay loam soil of the Indian Himalayas under different tillage and crop regimes. Agric. Ecosyst. Environ. 132 (1–2), 126–134. https://doi.org/10.1016/j.agee.2009.03.007.

Biddoccu, M., Ferraris, S., Pitacco, A., Cavallo, E., 2017. Temporal variability of soil management effects on soil hydrological properties, runoff and erosion at the field scale in a hillslope vineyard, North-West Ital. Soil Tillage Res. 165, 46–58. https://doi.org/10.1016/j.still.2016.07.017.

Bogunović, I., Pereira, P., Kisić, I., Sajko, K., Sraka, M., 2018. Tillage management impacts on soil compaction, erosion and crop yield in Stagnosols (Croatia). Catena 160, 376–384. https://doi.org/10.1016/j.catena.2017.10.009.

Bormann, H., Klaassen, K., 2008. Seasonal and land use dependent variability of soil hydraulic and soil hydrological properties of two northern German soils. Geoderma 145 (3-4), 295–302. https://doi.org/10.1016/j.geoderma.2008.03.017.

Borrelli, P., Van, K.O., Meusburger, K., Alewell, C., Lugato, E., Panagos, P., 2018. A step towards a holistic assessment of soil degradation in Europe: coupling on-site erosion with sediment transfer and carbon fluxes. Environ. Res. 161, 291–298. https://doi.org/10.1016/j.envres.2017.11.009.

Breshears, D.D., 2010. Wind and water erosion and transport in semi-arid shrubland, grassland and forest ecosystems: quantifying dominance of horizontal wind-driven transport. Earth Surf. Process. Landf. 28 (11), 1189–1209. https://doi.org/10.1002/esp.1034.

Bryan, R.B., 2000. Soil erodibility and processes of water erosion on hillslope. Geomorphology 32 (3), 385–415. https://doi.org/10.1016/s0169555x(99)00105-1.

Bryant, D.M., Holland, E.A., Seastedt, T.R., Walker, M.D., 1998. Analysis of litter decomposition in an alpine tundra. Can. J. Bot. 76 (7), 1295–1304. https://doi.org/10.1139/b98-117.

Chahine, M.T., 1992. The hydrological cycle and its influence on climate. Nature 359 (6394), 373–380. https://doi.org/10.1038/359373a0.

Chen, C., Wagenet, R.J., 1992. Simulation of water and chemicals in macropore soils. Part 1. Representation of the equivalent macropore influence and its effect on soil water flow. J. Hydrol. (Amst) 130, 105–126. https://doi.org/10.1016/0022-1694(92)90106-6.

Choudhary, M.A., Lal, R., Dick, W.A., 1997. Long-term tillage effects on runoff and soil erosion under simulated rainfall for a central Ohio soil. Soil Tillage Res. 42 (3), 175–184. https://doi.org/10.1016/s0167-1987(97)00005-00006.

Cournane, F.C., McDowell, R., Littlejohn, R., Condron, L., 2011. Effects of cattle, sheep and deer grazing on soil physical quality and losses of phosphorus and suspended sediment losses in surface runoff. Agric. Ecosyst. Environ. 140 (1–2), 264–272. https://doi.org/10.1016/j.agee.2010.12.013.

Denef, K., Six, J., Merckx, R., Paustian, K., 2002. Short-term effects of biological and physical forces on aggregate formation in soils with different clay mineralogy. Plant Soil 246 (2), 185–200. https://doi.org/10.1023/A:1020668013524.

Doetterl, S., Oost, K.V., Six, J., 2012. Towards constraining the magnitude of global agricultural sediment and soil organic carbon fluxes. Earth Surf. Process. Landf. 37 (6), 642–655. https://doi.org/10.1002/esp.3198.

Dong, Y., Wu, Y., Qin, W., Guo, Q., Yin, Z., Duan, X., 2019. The gully erosion rates in the black soil region of northeastern China: induced by different processes and indicated by different indexes. Catena 182, 104146. https://doi.org/10.1016/j.catena.2019.104146.

Garciapausas, J., Casals, P., Camarero, L., Huguet, C., Thompson, R., Sebastià, M.T., 2008. Factors regulating carbon mineralization in the surface and subsurface soils of Pyrenean mountain grasslands. Soil Biol. Biochem. 40 (11), 2803–2810. https://doi.org/10.1016/j.soilbio.2008.08.001.

Gu, Z., Xie, Y., Gao, Y., Ren, X., Cheng, C., Wang, S., 2018. Quantitative assessment of soil productivity and predicted impacts of water erosion in the black soil region of northeastern china. Sci. Total Environ. 637-638, 706–716. https://doi.org/10.1016/j.scitotenv.2018.05.061.

Haghighi, F., Gorji, M., Shorafa, M., 2010. A study of the effects of land use changes on soil physical properties and organic matter. Land Degrad. Dev. 21 (5), 496–502. https://doi.org/10.1002/ldr.999.

Harden, J.W., Sharpe, J.M., Parton, W.J., Ojima, D.S., Fries, T.L., Huntington, T.G., et al., 1999. Dynamic replacement and loss of soil carbon on eroding cropland. Global Biogeochem. Cycles 13 (4), 885–901. https://doi.org/10.1029/1999gb900061.

Hartmann, P., Fleige, H., Horn, R., 2009. Physical properties of forest soils along a fly-ash deposition gradient in northeast Germany. Geoderma 150 (1-2), 189–195. https://doi.org/10.1016/j.geoderma.2009.02.005.

Hendrix, P.F., Mueller, B.R., Bruce, R.R., Langdale, G.W., Parmelee, R.W., 1992. Abundance and distribution of earthworms in relation to landscape factors on the georgia piedmont. U.S.A. Soil Biology and Biochemistry 24 (12), 1357–1361. https://doi.org/10.1016/00380717(92)90118-h.

Hong, C., Liu, C., Li, J., Zou, X., Bo, L., Kang, L., 2017. Wind erosion mass variability with sand bed in a wind tunnel. Soil Tillage Res. 165, 181–189. https://doi.org/10.1016/j.still.2016.08.013.

Hu, G., Wu, Y.Q., Liu, B.Y., Zheng, Q.H., Zhang, Y.G., Liu, H.H., 2007. The growth characteristics of gully Erosion over rolling hilly black soil area of Northeast China. Acta Geographica Sinica 62 (11), 1165–1173 (in Chinese).

Islam, K.R., Weil, R.R., 2000. Land use effects on soil quality in a tropical forest ecosystem of bangladesh. Agric. Ecosyst. Environ. 79 (1), 9–16. https://doi.org/10.1016/s0167-8809(99)00145-0.

Jiang, H., Han, X., Zou, W., Hao, X., Zhang, B., 2018. Seasonal and long-term changes in soil physical properties and organic carbon fractions as affected by manure application rates in the Mollisol region of Northeast China. Agric. Ecosyst. Environ. 268, 133–143. https://doi.org/10.1016/j.agee.2018.09.00.

Jiang, Y., Zheng, F., Wen, L., Shen, H.O., 2019. Effects of sheet and rill erosion on soil aggregates and organic carbon losses for a Mollisol hillslope under rainfall simulation. J. Soils Sediments 19 (1), 467–477. https://doi.org/10.1007/s11368-018-2043-y.

Klute, A., Dirksen, C., 1986. Methods of soil analysis, part 1: physical and mineralogical methods, 2nd edition. In: Klute, A. (Ed.), Hydraulic Conductivity and Diffusivity: Laboratory Methods. American Society of Agronomy, Madison, WI, pp. 687–734.

Kume, T., Takizawa, H., Yoshifuji, N., Tanaka, K., Tantasirin, C., Tanaka, N., Suzuki, M., 2007. Impact of soil drought on sap flow and water status of evergreen trees in a tropical monsoon forest in northern Thailand. For. Ecol. Manage. 238 (1–3), 220–230. https://doi.org/10.1016/j.foreco.2006.10.019.

Lado, M., Benhur, M., Shainberg, I., 2004. Soil wetting and texture effects on aggregate stability, seal formation, and erosion. Soil Sci. Soc. Am. J. 68 (6), 1992–1999. https://doi.org/10.2136/sssaj2004.1992.

Lal, R., 2001. Soil degradation by erosion. Land Degrad. Dev. 12 (6), 519–539. https://doi.org/10.1002/ldr.472.

Larson, W.E., Padilla, W.A., 1990. Physical properties of a mollisol, an oxisol and an inceptisol. Soil Tillage Res. 16 (1–2), 23–33. https://doi.org/10.1016/0167-1987(90)90019-a.

Le Bissonnais, Y., 1996. Aggregate stability and assessment of soil crustability and erodibility: I. Theory and methodology. Eur. J. Soil Sci. 48 (1), 39–48. https://doi.org/10.1111/j.1365-2389.1996.tb01843.x.

Letey, J., Levy, G.J., Mamedov, A.I., Shainberg, I., 2001. Wetting rate, sodicity, and soil texture effects on infiltration rate and runoff. Soil Res. 39 (6), 1293–1305. https://doi.org/10.1071/sr01029.

Li, Q.Y., Fang, H.Y., Sun, L.Y., Cai, Q.G., 2012. Using the ^{137}Cs technique to study the effect of soil redistribution on soil organic carbon and total nitrogen stocks in a agricultural catchment of Northeast China. Land Degrad. Dev. 25 (4), 350–359. https://doi.org/10.1002/ldr.2144.

Li, T.C., Shao, M.A., Jia, Y.H., 2016. Application of X-ray tomography to quantify macropore characteristics of Loess soil under two perennial plants. Eur. J. Soil Sci. 65 (3), 266–275. https://doi.org/10.1111/ejss.12330.

Li, T.C., Shao, M.A., Jia, Y.H., Jia, X.X., Huang, L.M., 2018. Small-scale observation on the effects of the burrowing activities of mole crickets on soil erosion and hydrologic processes. Agric. Ecosyst. Environ. 261, 136–143. https://doi.org/10.1016/j.agee.2018.04.010.

Li, H., Liao, X., Zhu, H., Wei, X., Shao, M., 2019. Soil physical and hydraulic properties under different land uses in the black soil region of Northeast China. Can. J. Soil Sci. 99 (4), 406–419. https://doi.org/10.1139/cjss-2019-0039.

Li, H., Zhu, H., Qiu, L., Wei, X., Liu, B., Shao, M., 2020. Response of soil OC, N and P to land-use change and erosion in the black soil region of the Northeast China. Agric. Ecosyst. Environ. 302, 107081 https://doi.org/10.1016/j.agee.2020.107081.

Logsdon, S.D., 2013. Depth dependence of chisel plow tillage erosion. Soil Tillage Res. 128, 119–124. https://doi.org/10.1016/j.still.2012.06.014.

Ma, R.M., Li, Z.X., Cai, C.F., Wang, J.G., 2014. The dynamic response of splash erosion to aggregate mechanical breakdown through rainfall simulation events in Ultisols (subtropical China). Catena 121, 279–287. https://doi.org/10.1016/j.catena.2014.05.028.

Mamedov, A.I., Levy, G.J., 2001. Clay dispersivity and aggregate stability effects on seal formation and erosion in effluent-irrigated soils. Soil Sci. 166 (9), 631–639. https://doi.org/10.1097/00010694-200109000-00007.

Manyevere, A., Muchaonyerwa, P., Mnkeni, P.N.S., Laker, M.C., 2016. Examination of soil and slope factors as erosion controlling variables under varying climatic conditions. Catena 147, 245–257. https://doi.org/10.1016/j.catena.2016.06.035.

Markus, D., 2008. The history of soil erosion and fluvial deposits in small catchments of central Europe: deciphering the long-term interaction between humans and the environment-A review. Geomorphology 101 (1–2), 192–208. https://doi.org/10.1016/j.geomorph.2008.05.023.

McDonald, M.A., Healey, J.R., Stevens, P.A., 2002. The effects of secondary forest clearance and subsequent land-use on erosion losses and soil properties in the Blue Mountains of Jamaica. Agric. Ecosyst. Environ. 92 (1), 1–19. https://doi.org/10.1016/s01678809(01)00286-00289.

Nagumo, F., Issaka, R.N., Hoshikawa, A., 2006. Effects of tillage practices combined with mucuna fallow on soil erosion and water dynamics on Ishigaki island, Japan. Soil Sci. Plant Nutr. 52 (6), 676–685. https://doi.org/10.1111/j.1747-0765.2006.00095.x.

Nelson, D.W., Sommers, L.E., Sparks, D.L., Page, A.L., Helmke, P.A., Loeppert, R.H., Soltanpour, P.N., Tabatabai, M.A., Johnston, C.T., Sumner, M.E., 1996. Total carbon, organic carbon, and organic matter. Methods Soil Anal. 9, 961–1010. https://doi.org/10.2136/sssabookser5.3.c34.

Nie, X., Li, Z., Huang, J., Liu, L., Xiao, H., Liu, C., 2018. Thermal stability of organic carbon in soil aggregates as affected by soil erosion and deposition. Soil Tillage Res. 175, 82–90. https://doi.org/10.1016/j.still.2017.08.010.

Onet, A., Dincă, L.C., Grenni, P., Laslo, V., Teusdea, A.C., Vasile, D.L., 2019. Biological indicators for evaluating soil quality improvement in a soil degraded by erosion processes. J. Soils Sediments 19 (5), 2393–2404. https://doi.org/10.1007/s11368-018-02236-02239.

Opara, C.C., 2009. Soil microaggregates stability under different land use types in Southeastern Nigeria. Catena 79 (2), 103–112. https://doi.org/10.1016/j.catena.2009.06.001.

Osman, Towhid K., 2013. Soil Degradation, Conservation and Remediation. Springer, Netherlands.

Ouyang, W., Wu, Y., Hao, Z., Zhang, Q., Bu, Q., Gao, X., 2018. Combined impacts of land use and soil property changes on soil erosion in a Mollisol area under long-term agricultural development. Sci. Total Environ. 613, 798–809. https://doi.org/10.1016/j.scitotenv.2017.09.173.

Qiu, Y., Fu, B., Wang, J., Chen, L., 2001. Spatial variability of soil moisture content and its relation to environmental indices in a semi-arid gully catchment of the Loess Plateau, China. J. Arid Environ. 49 (4), 723–750. https://doi.org/10.1006/jare.2001.0828.

Qiu, L.P., Zhang, Q., Zhu, H.S., Reich, Peter B., Banerjee, S., van der Heijden, Marcel G. A., Sadowsky, Michael J., Ishii, S., Jia, X.X., Shao, M.A., Liu, B.Y., Jiao, H., Li, H.Q., Wei, X.R., 2021a. Erosion reduces soil microbial diversity, network complexity and multifunctionality. ISME J. https://doi.org/10.1038/s41396-021-00913-1.

Qiu, L.P., Zhu, H.S., liu, J., Yao, Y.F., Wang, X., Rong, G.H., Zhao, X.N., Shao, M.A., Wei, X.R., 2021b. Soil erosion significantly reduces organic carbon and nitrogen mineralization in a simulated experiment. Agric. Ecosyst. Environ. 307, 107232 https://doi.org/10.1016/j.agee.2020.107232.

Reatto, A., Da Silva, E.M., Bruand, A., Martins, E.S., Lima, J.E.F.W., 2008. Validity of the centrifuge method for determining the water retention properties of tropical soils. Soil Sci. Soc. Am. J. 72 (6), 1547–1553. https://doi.org/10.2136/sssaj2007.0355n.

Reganold, J.P., Elliott, L.F., Unger, Y.L., 1987. Long-term effects of organic and conventional farming on soil erosion. Nature 330 (6146), 370–372. https://doi.org/10.1038/330370a0.

Rehder, H., 1995. Soil compaction processes and their effects on the structure of arable soils and the environment. Soil Tillage Res. 35 (1–2), 23–36. https://doi.org/10.1016/0167-1987(95)00479-c.

Reichert, J.M., Bervald, C.M.P., Rodrigues, M.F., Kato, O.R., Reinert, D.J., 2014. Mechanized land preparation in eastern Amazon in fire-free forest-based fallow systems as alternatives to slash-and-burn practices: hydraulic and mechanical soil properties. Agric. Ecosyst. Environ. 192, 47–60. https://doi.org/10.1016/j.agee.2014.03.046.

Risch, A.C., Jurgensen, M.F., Frank, D.A., 2007. Effects of grazing and soil micro-climate on decomposition rates in a spatio-temporally heterogeneous grassland. Plant Soil 298 (1–2), 191–201. https://doi.org/10.1007/s11104-007-9354-x.

Sanford, G.R., Posner, J.L., Schuler, R.T., Baldock, J.O., 2008. Effect of dairy slurry application on soil compaction and corn (*zea mays* L.) yield in southern Wisconsin. Soil Tillage Res. 100 (1–2), 42–53. https://doi.org/10.1016/j.still.2008.04.003.

Sarapatka, B., Cap, L., Bila, P., 2018. The varying effect of water erosion on chemical and biochemical soil properties in different parts of Chernozem slopes. Geoderma 314, 20–26. https://doi.org/10.1016/j.geoderma.2017.10.037.

Scheffler, R., Neill, C., Krusche, A.V., Elsenbeer, H., 2011. Soil hydraulic response to land-use change associated with the recent soybean expansion at the Amazon agricultural frontier. Agric. Ecosyst. Environ. 144 (1), 281–289. https://doi.org/10.1016/j.agee.2011.08.016.

Sharma, R.B., Verma, G.P., 1977. Characterization of shrinkage cracks in medium black clay soil of madhya pradesh. Plant Soil 48 (2), 323–333. https://doi.org/10.1007/bf02187244.

Six, J., Elliott, E.T., Paustian, K., Doran, J.W., 1998. Aggregation and soil organic matter accumulation in cultivated and native grassland soils. Soil Sci. Soc. Am. J. 62 (5), 1367–1377. https://doi.org/10.2136/sssaj1998.03615995006200050.

Sobieraj, J., Elsenbeer, H., Coelho, R., Newton, B., 2002. Spatial variability of soil hydraulic conductivity along a tropical rainforest catena. Geoderma 108 (1-2), 79–90. https://doi.org/10.1016/s00167061(02)00122-2.

Stallard, R., 1998. Terrestrial sedimentation and the carbon cycle: coupling weathering and erosion to carbon burial. Global Biogeochem. Cycles 12 (2), 231–257. https://doi.org/10.1029/98gb00741.

Thomaz, Edivaldo E.L., 2017. Ash physical characteristics affects differently soil hydrology and erosion subprocesses. Land Degrad. Dev. 29 (3), 690–700. https://doi.org/10.1002/ldr.2715.

Tuo, D.F., Xu, M.X., Gao, G.Y., 2018. Relative contributions of wind and water erosion to total soil loss and its effect on soil properties in sloping croplands of the Chinese Loess Plateau. Sci. Total Environ. 633, 1032–1040. https://doi.org/10.1016/j.scitotenv.2018.03.237.

USDA, 1975. Soil Taxonomy: a Basic System of Soil Classification for Making and Interpreting Soil Survey. United States Department of Agriculture. Govt. Printing Office, Washington, DC.

Wagner, S., Cattle, S.R., Scholten, T., 2010. Soil-aggregate formation as influenced by clay content and organic-matter amendment. J. Plant Nutr. Soil Sci. 170 (1), 173–180. https://doi.org/10.1002/jpln.200521732.

Wang, L., Shi, Z.H., 2015. Size selectivity of eroded sediment associated with soil texture on steep slopes. Soil Sci. Soc. Am. J. 79 (3), 917–929. https://doi.org/10.2136/sssaj2014.10.0415.

Wang, X., Cammeraat, L.H., Wang, Z., Zhou, J., Govers, G., Kalbitz, K., 2013. Stability of organic matter in soils of the Belgian Loess Belt upon erosion and deposition. Eur. J. Soil Sci. 64 (2), 219–228. https://doi.org/10.1111/ejss.12018.

Wang, Z.Y., Silva, L.C.R., Sun, G., Luo, P., Mou, C.X., Horwath, W.R., 2015a. Quantifying the impact of drought on soil-plant interactions: a seasonal analysis of biotic and abiotic controls of carbon and nutrient dynamics in high-altitudinal grasslands. Plant Soil 389 (1–2), 59–71. https://doi.org/10.1007/s11104-014-2337-2339.

Wang, Y.Q., Shao, M.A., Han, X.W., Liu, Z.P., 2015b. Spatial variability of soil parameters of the van Genuchten model at a regional scale. Clean-Soil, Air, Water 43 (2), 271–278. https://doi.org/10.1002/clen.201300903.

Wang, Y., Wei, Y., Fan, J., Mu, J., Wei, X., Wang, Q., 2018. Effects of subsequent rainfall events with different intensities on runoff and erosion in a coarse soil. Catena 170, 100–107. https://doi.org/10.1016/j.catena.2018.06.008.

Wei, S., Zhang, X., Mclaughlin, N.B., Chen, X., Jia, S., Liang, A., 2017. Impact of soil water erosion processes on catchment export of soil aggregates and associated SOC. Geoderma 294, 63–69. https://doi.org/10.1016/j.geoderma.2017.01.021.

Wilkinson, G.E., Klute, A., 1959. Some tests of the similar media concept of capillary flow: II. Flow systems data. Soil Sci. Soc. Am. J. 23 (6), 434–437. https://doi.org/10.2136/sssaj1959.03615995002300060.

Wirtz, S., Seeger, M., Ries, J.B., 2012. Field experiments for understanding and quantification of rill erosion processes. Catena 91 (5), 20–34. https://doi.org/10.1016/j.catena.2010.12.002.

Wu, Y., Zheng, Q., Zhang, Y., Liu, B., Cheng, H., Wang, Y., 2008. Development of gullies and sediment production in the black soil region of northeastern China. Geomorphology 101 (4), 683–691. https://doi.org/10.1016/j.geomorph.2008.03.008.

Xiao, L., Yuan, G., Feng, L., Bi, D., Wei, J., 2020. Soil properties and the growth of wheat (Triticum aestivum L.) and maize (Zea mays L.) in response to reed (phragmites communis) biochar use in a salt-affected soil in the Yellow River Delta. Agric. Ecosyst. Environ. 303, 107124 https://doi.org/10.1016/j.agee.2020.107124.

Yadav, V., Malanson, G.P., 2009. Modeling impacts of erosion and deposition on soil organic carbon in the big creek basin of southern Illinois. Geomorphology 106 (3-4), 300–314. https://doi.org/10.1016/j.geomorph.2008.11.011.

Yan, F.L., Shi, Z.H., Li, Z.X., Cai, C.F., 2008. Estimating interrill soil erosion from aggregate stability of Ultisols in subtropical China. Soil Tillage Res. 100 (1–2), 34–41. https://doi.org/10.1016/j.still.2008.04.006.

Yang, J., Xu, X., Liu, M., Xu, C., Zhang, Y., Luo, W., Wang, K., 2017. Effects of “Grain for Green” program on soil hydrologic functions in karst landscapes, southwestern China. Agric. Ecosyst. Environ. 247, 120–129. https://doi.org/10.1016/j.agee.2017.06.025.

Zhang, Y., Wu, Y., Liu, B., Zheng, Q., Yin, J., 2007. Characteristics and factors controlling the development of ephemeral gullies in cultivated catchments of black soil region, Northeast China. Soil Tillage Res. 96 (1–2), 28–41. https://doi.org/10.1016/j.still.2007.02.010.

Zhao, H.L., Zhao, X.Y., Zhou, R.L., Zhang, T.H., Drake, S., 2005. Desertification processes due to heavy grazing in sandy rangeland, Inner Mongolia. J. Arid Environ. 62 (2), 309–319. https://doi.org/10.1016/j.jaridenv.2004.11.009.

Zhao, L., Sun, Y., Zhang, X., Yang, X., Drury, C.F., 2006a. Soil organic carbon in clay and silt sized particles in Chinese Mollisols: relationship to the predicted capacity. Geoderma 132 (3-4), 310–323. https://doi.org/10.1016/j.geoderma.2005.04.026.

Zhao, H.L., Yi, X.Y., Zhou, R.L., Zhao, X.Y., Zhang, T.H., Drake, S., 2006b. Wind erosion and sand accumulation effects on soil properties in Horqin Sandy Farmland. Inner Mongolia. Catena 65 (1), 70–79. https://doi.org/10.1016/j.catena.2005.10.001.

Zhao, P., Li, S., Wang, E., Chen, X., Deng, J., Zhao, Y., 2018. Tillage erosion and its effect on spatial variations of soil organic carbon in the black soil region of China. Soil Tillage Res. 178, 72–81. https://doi.org/10.1016/j.still.2017.12.022.

Zibilske, L.M., Materon, L.A., 2005. Biochemical properties of decomposing cotton and corn stem and root residues. Soil Sci. Soc. Am. J. 69 (2), 378–386. https://doi.org/10.2136/sssaj2005.0378.